JEM

Supplemental material

Zhu et al., https://doi.org/10.1084/jem.20190337

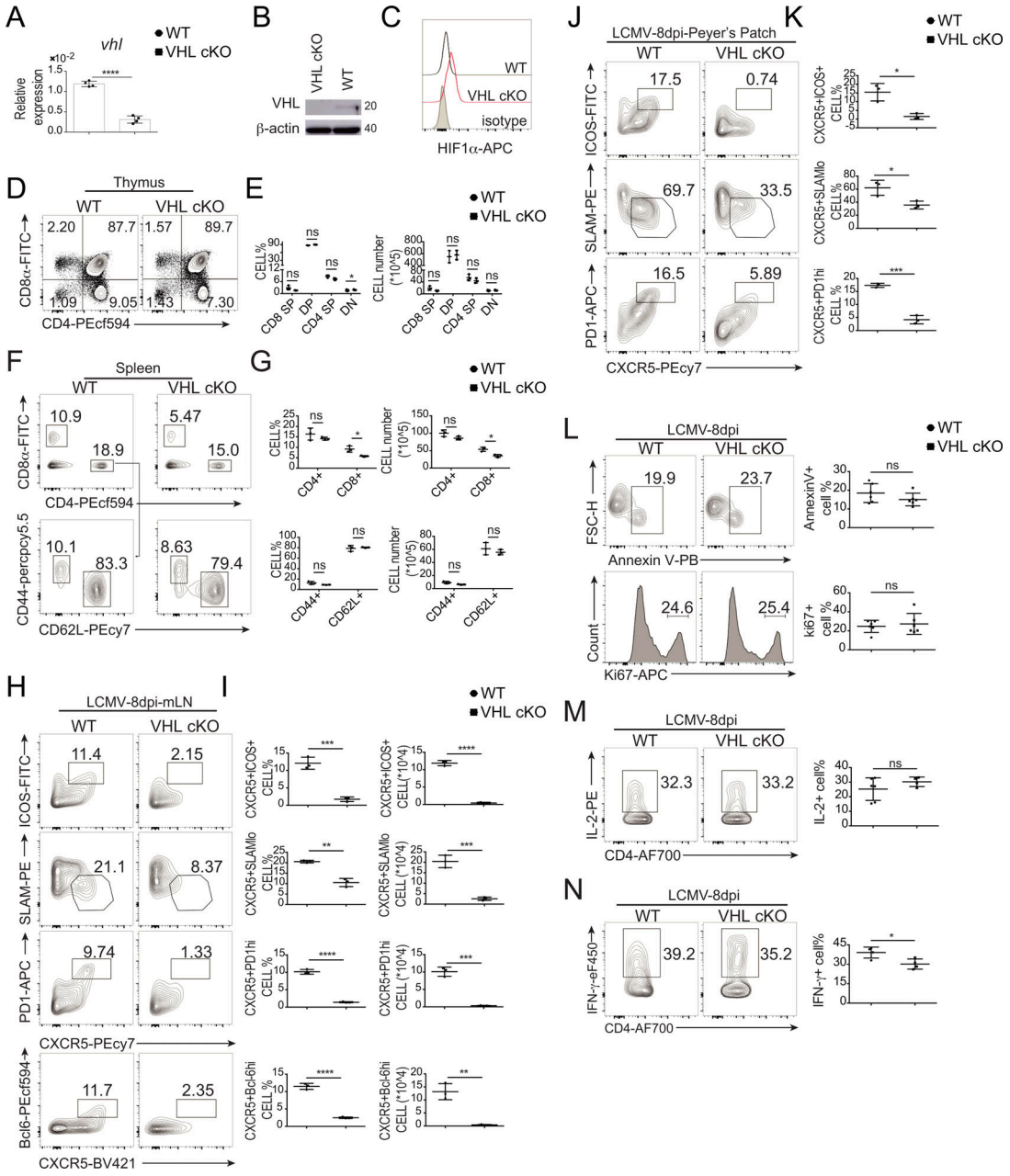

Figure S1. **VHL positively regulates the development of Tfh cells.** Related to Fig. 1. **(A)** qRT-PCR analysis of mRNA of *vhl* in splenic CD4$^+$ T cells from WT and *CD4^{cre}Vhl$^{fl/fl}$* (VHL cKO) mice; gene expression was normalized to that of *Actb* mRNA. **(B)** Immunoblotting analysis of VHL expression in splenic CD4$^+$ T cells from WT and VHL cKO mice. **(C)** Representative flow-cytometric analysis of HIF-1α expression in WT and VHL cKO CD4$^+$ T cells stimulated with anti-CD3 and anti-CD28 for 24 h. **(D)** Representative flow-cytometric plots of CD4$^+$ or CD8$^+$ T cells in the thymus from WT and VHL cKO mice. Numbers adjacent to outlined areas indicate frequency of CD8$^+$CD4$^-$ single positive (CD8$^+$ SP), CD4$^+$CD8$^+$ double positive (DP), CD8$^-$CD4$^+$ (CD4$^+$ SP), or CD4$^-$CD8$^-$ double negative (DN) thymocytes. **(E)** Quantification of frequency and number of CD8$^+$ SP, DP, CD4$^+$ SP, and DN thymocytes as in D (*n* = 3 per group). **(F)** Representative flow-cytometric plots of CD4$^+$ or CD8$^+$ T cells in the spleen from WT and VHL cKO mice. Numbers adjacent to outlined areas indicate frequency of CD4$^+$ or CD8$^+$ T cells (top row), CD4$^+$CD62L$^+$CD44$^-$ naive T cells, or CD4$^+$CD62L$^-$CD4$^+$ effector T cells (bottom row). **(G)** Quantification of frequency and number of indicated T cell subsets in the spleen of mice as in F (*n* = 3 per group). **(H)** Representative flow-cytometric plots of CD44$^+$CD4$^+$ T cells in mLN from WT and VHL cKO mice 8 d after infection with LCMV. Numbers adjacent to outlined areas indicate frequency of Tfh (CXCR5$^+$ICOS$^+$ or CXCR5$^+$SLAM^{lo}) cells or GC-Tfh (CXCR5$^+$PD-1^{hi} or CXCR5$^+$Bcl-6^{hi}) cells. **(I)** Quantification of frequency (among CD44$^+$CD4$^+$ T cells) and number of Tfh and GC-Tfh cells in mLN of mice as in H (*n* = 3 per group). **(J)** Representative flow-cytometric plots of CD44$^+$CD4$^+$ T cells in PP from WT and VHL cKO mice 8 d after LCMV infection. Numbers adjacent to outlined areas indicate frequency of Tfh (CXCR5$^+$ICOS$^+$ or CXCR5$^+$SLAM^{lo}) cells or GC-Tfh (CXCR5$^+$PD-1^{hi}) cells. **(K)** Quantification of frequency (among CD44$^+$CD4$^+$ T cells) of Tfh cells and GC-Tfh cells in PP of mice as in J (*n* = 3 per group). **(L–N)** Left: Representative flow-cytometric analysis of CD44$^+$CD4$^+$ T cells in the spleen from WT and VHL cKO mice 8 d after LCMV infection. Numbers adjacent to outlined areas indicate frequency of AnnexinV$^+$ dead cells (top row) and Ki67$^+$ proliferating cells (bottom row) (L), IL-2–producing cells (M) or IFN-γ–producing cells (N). Right: Quantification of frequency of indicated CD44$^+$CD4$^+$ T cells in the spleen of mice as in L–N (*n* = 4–6 per group). Each symbol (E, G, I, K–N) represents an individual mouse; small horizontal lines indicate the mean (± SD). *, P < 0.05; **, P < 0.01; ***, P < 0.001; ****, P < 0.0001; ns, nonsignificant (Student's *t* test). Data are representative of three independent experiments. FSC-H, forward scatter height.

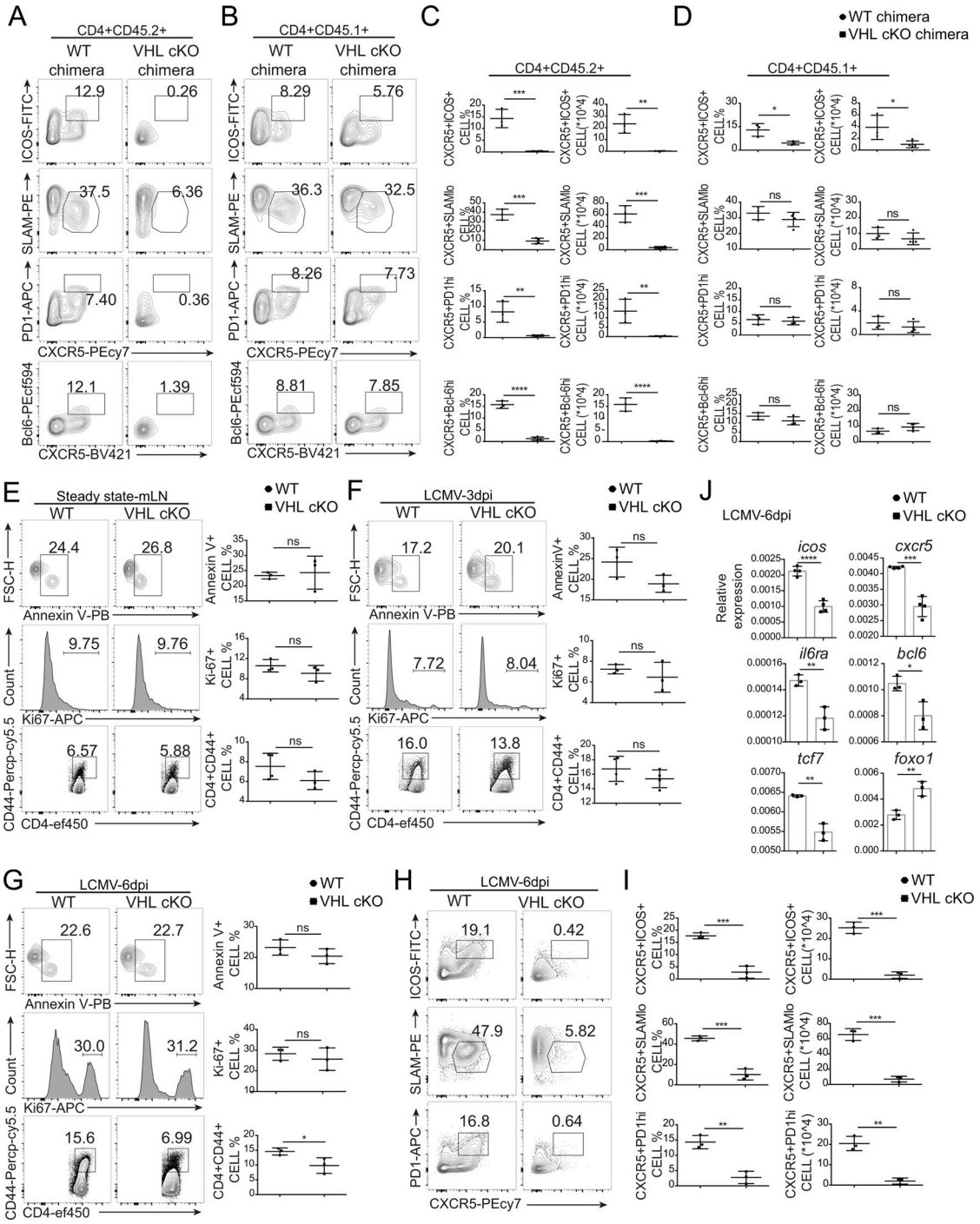

Figure S2. **VHL intrinsically regulates the early development of Tfh cells without affecting cell death and proliferation.** Related to Figs. 2 and 3. **(A and B)** Representative flow-cytometric plots of donor CD45.2$^+$ (A) or CD45.1$^+$ control (B) CD4$^+$CD44$^+$ T cells in the spleen from mixed bone marrow chimeras reconstituted for 6–8 wk with WT or VHL cKO (CD45.2$^+$) and WT CD45.1$^+$ bone marrow cells followed by LCMV infection. Numbers adjacent to outlined areas indicate frequency of Tfh (CXCR5$^+$ICOS$^+$ or CXCR5$^+$SLAM^{lo}) cells or GC-Tfh (CXCR5$^+$PD-1^{hi} or CXCR5$^+$Bcl-6^{hi}) cells. **(C and D)** Quantification of frequency and number of CD45.2$^+$ (C) or CD45.1$^+$ (D) CD4$^+$CD44$^+$ Tfh and GC-Tfh cells of mice as in A and B (n = 3 or 4 per group). **(E–G)** Left: Representative flow-cytometric analysis of CD4$^+$ T cells from WT and VHL cKO mice under steady state (E), 3 d after LCMV infection (F), or 6 d after LCMV infection (G). Numbers adjacent to outlined areas indicate frequency of Annexin V$^+$ dead cells (top row), Ki67$^+$proliferating cells (middle row), and CD44$^+$ activated cells (bottom row). Right: Quantification of frequency of indicated CD4$^+$ T cells from mice as in E–G (n = 3 per group). **(H)** Representative flow-cytometric plots of CD44$^+$CD4$^+$ T cells in the spleen from WT and VHL cKO mice 6 d after infection with LCMV. Numbers adjacent to outlined areas indicate frequency of Tfh (CXCR5$^+$ICOS$^+$ or CXCR5$^+$SLAM^{lo}) cells or GC-Tfh (CXCR5$^+$PD-1^{hi}) cells. **(I)** Quantification of frequency (among CD44$^+$CD4$^+$ T cells) and number of Tfh or GC-Tfh cells of mice as in H (n = 3 or 4 per group). **(J)** RT-PCR analysis of mRNA of Tfh cell–related genes in CD44$^+$CD4$^+$ T cells from WT and VHL cKO mice 6 d after LCMV infection; results were normalized to those of *Actb* mRNA (encoding β-actin). Each symbol (C–G, I) represents an individual mouse; small horizontal lines indicate the mean (± SD). *, P < 0.05; **, P < 0.01; ***, P < 0.001; ****, P < 0.0001; ns, nonsignificant (Student's t test). Data are representative of three independent experiments.

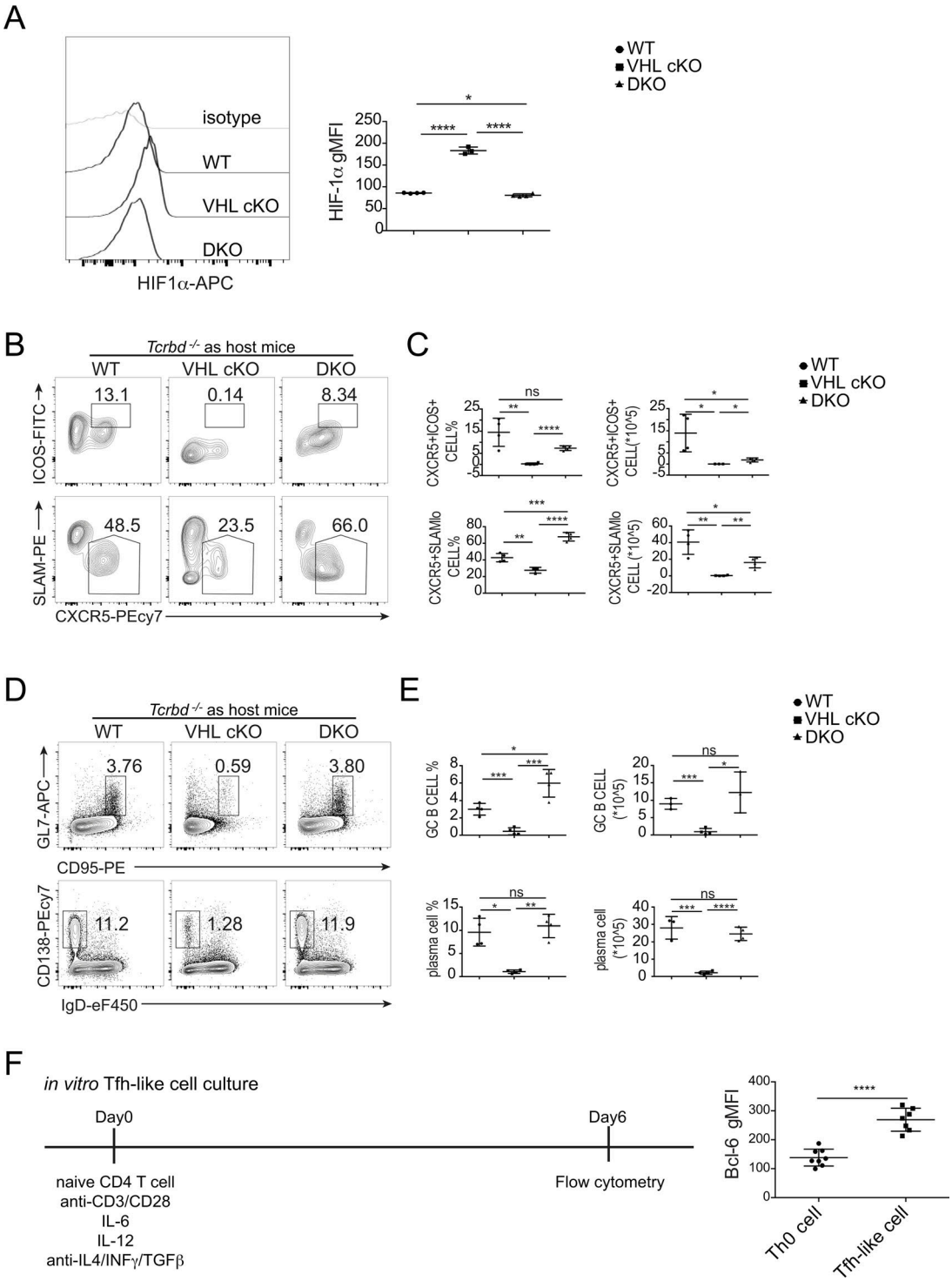

Figure S3. **Rescue by HIF-1α deficiency.** Related to Fig. 4. **(A)** Representative flow-cytometric analysis of HIF-1α expression (left) and quantification of HIF-1α MFI (right) in WT, VHL cKO, and *Vhl*$^{fl/fl}$*Hif1a*$^{fl/fl}$*CD4*^{Cre} (DKO) CD4$^+$ T cells stimulated with anti-CD3 and anti-CD28 for 24 h. **(B)** Representative flow-cytometric plots of donor CD45.2$^+$CD4$^+$ T cells obtained from *Tcrbd*$^{-/-}$ host mice receiving naive CD4$^+$ T cells from WT, VHL cKO, and DKO SMARTA donor mice, followed by infection with LCMV and analysis 8 d after infection. Numbers adjacent to outlined areas indicate frequency of Tfh (CXCR5$^+$ICOS$^+$ or CXCR5$^+$SLAM^{lo}) cells. **(C)** Quantification of frequency (among CD45.2$^+$CD4$^+$ T cells) and number (CD45.2$^+$CD4$^+$) of Tfh cells of *Tcrbd*$^{-/-}$ host mice as in B (n = 3 or 4 per group). **(D)** Representative flow-cytometric plots of total B220$^+$ B cells obtained from *Tcrbd*$^{-/-}$ host mice as described in B. Numbers adjacent to outlined areas indicate frequency of GC B (GL7$^+$CD95$^+$) cells (top row) or plasma CD138$^+$IgD^{lo} cells (bottom row) in the spleen. **(E)** Quantification of frequency (among B220$^+$ B cells) and number of GC B and plasma cells in the spleen of mice as in B (n = 3 or 4 per group). **(F)** Workflow of in vitro Tfh-like cell culture system (left). Quantification of Bcl-6 MFI (right) in T helper type 0 cells or Tfh-like cells. Each symbol (C and E) represents an individual mouse; small horizontal lines indicate the mean (± SD). *, P < 0.05; **, P < 0.01; ***, P < 0.001; ****, P < 0.0001; ns, nonsignificant (Student's t test). Data are representative of three independent experiments.

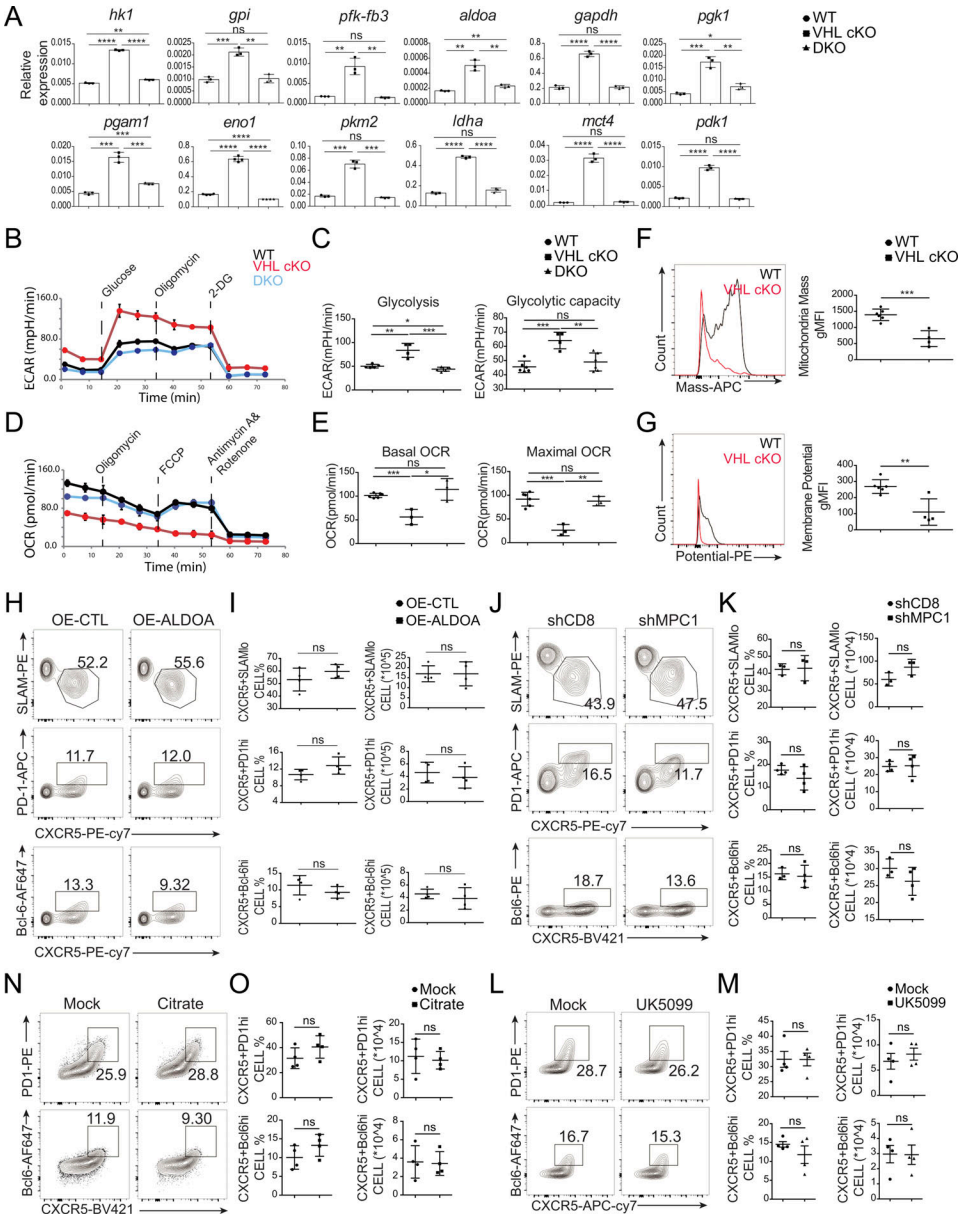

Figure S4. **HIF-1α–dependent up-regulation of glycolysis and attenuated oxidative metabolism in VHL cKO cells.** Related to Fig. 5. **(A)** qRT-PCR analysis of glycolytic gene expression in CD44$^+$CD4$^+$ T cells from WT, VHL cKO, and DKO mice 8 d after LCMV infection (n = 4 per group); each gene expression was normalized to that of *Actb* mRNA. **(B)** Seahorse traces for ECAR of in vitro activated CD4$^+$ T cells by anti-CD3 and anti-CD28 from WT, VHL cKO, or DKO mice. **(C)** Quantification of measures of glycolysis (left) and glycolytic capacity (right) of activated CD4$^+$ T cells from WT, VHL cKO, or DKO mice as in B. **(D)** Seahorse traces for OCR of in vitro activated CD4$^+$ T cells by anti-CD3 and anti-CD28 from WT, VHL cKO, or DKO mice. **(E)** Quantification of measures of basal OCR (left) and maximal OCR (right) of activated CD4$^+$ T cells from WT, VHL cKO, or DKO mice as in D. **(F)** Representative flow-cytometric analysis (left) and quantification of MFI (right) of mitochondrial mass in CD4$^+$CD44$^+$ T cells from LCMV-infected WT or VHL cKO mice. **(G)** Representative flow-cytometric analysis (left) and quantification of MFI (right) of mitochondrial membrane potential in CD4$^+$CD44$^+$ T cells as in F. **(H)** Representative flow-cytometric plots of donor SMARTA CD45.1$^+$GFP$^+$CD4$^+$ T cells obtained from B6 host mice receiving SMARTA CD4$^+$ T cells transduced with retroviral vector expressing GFP only (OE-CTL), or ALDOA (OE-ALDOA) followed by infection of host mice with LCMV and analysis 8 d after infection. Numbers adjacent to outlined areas indicate frequency of Tfh (CXCR5$^+$SLAM^{lo}) cells or GC-Tfh (CXCR5$^+$PD-1^{hi} or CXCR5$^+$Bcl-6^{hi}) cells. **(I)** Quantification of frequency (among CD4$^+$CD45.1$^+$GFP$^+$ T cells) and number (CD4$^+$CD45.1$^+$GFP$^+$) of Tfh and GC-Tfh cells in host mice as in H (n = 4 per group). **(J)** Representative flow-cytometric plots of donor SMARTA CD45.1$^+$Ametrine$^+$CD4$^+$ T cells obtained from B6 host mice receiving SMARTA CD4$^+$ T cells transduced with shCD8 or shMPC1 (Ametrine$^+$), followed by infection of host mice with LCMV and analysis 8 d after infection. Numbers adjacent to outlined areas indicate frequency of Tfh (CXCR5$^+$SLAM^{lo}) cells or GC-Tfh (CXCR5$^+$PD-1^{hi} or CXCR5$^+$Bcl-6^{hi}) cells. **(K)** Quantification of frequency (among CD4$^+$CD45.1$^+$Ametrine$^+$ T cells) and number (CD4$^+$CD45.1$^+$Ametrine$^+$) of Tfh and GC-Tfh cells in host mice as in J (n = 3 or 4 per group). **(L and N)** Representative flow-cytometric plots of donor OT-II CD45.1$^+$CD4$^+$ T cells obtained from B6 host mice receiving WT OT-II CD4$^+$ T cells cultured in the absence (Mock) or presence of UK5099 (L) or citrate (N) followed by immunization of host mice with OVA protein and analysis 7 d after immunization. Numbers adjacent to outlined areas indicate frequency of GC-Tfh (CXCR5$^+$PD-1^{hi} or CXCR5$^+$Bcl-6^{hi}) cells. **(M and O)** Quantification of frequency (among CD4$^+$CD45.1$^+$ T cells) and number (CD4$^+$CD45.1$^+$) of GC-Tfh cells in the popliteal LN of host mice as in L and N (n = 4 per group). Each symbol (F, G, I, K, M, and O) represents an individual mouse; small horizontal lines indicate the mean (± SD). *, P < 0.05; **, P < 0.01; ***, P < 0.001; ****, P < 0.0001; ns, nonsignificant (Student's t test). Data are representative of three independent experiments.

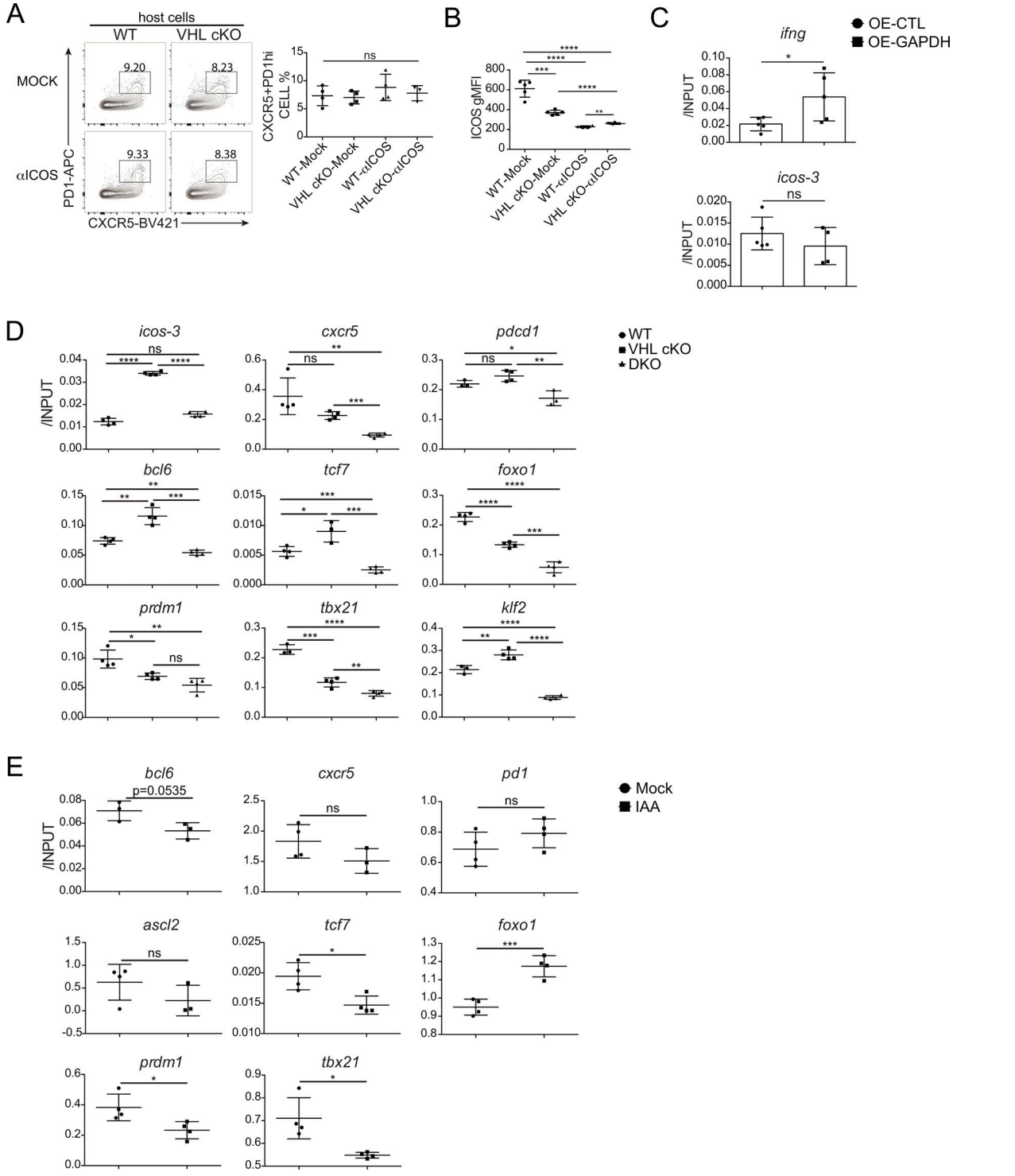

Figure S5. **GAPDH controls *icos* expression via m^{6}A modification.** Related to Figs. 6 and 7. **(A)** Representative flow-cytometric plots of host CD45.2$^+$CD4$^+$ T cells (left) and quantification of frequency (among CD45.2$^+$CD4$^+$ T cells) of GC-Tfh cells (right) obtained from B6 host mice receiving WT or VHL cKO OT-II CD4$^+$ T cells cultured in the absence or presence of anti-ICOS (C398.4A), followed by immunization with OVA protein and analysis 7 d after immunization. Numbers adjacent to outlined areas indicate frequency of CXCR5$^+$PD-1^{hi} GC-Tfh cells (n = 3 or 4 per group). **(B)** Quantification of ICOS MFI in WT or VHL cKO Tfh-like cells cultured in the absence or presence of anti-ICOS. **(C)** RIP–qRT-PCR analysis of binding of *icos* mRNA or *ifng* mRNA to GAPDH immunoprecipitated with anti-Myc antibody in WT CD4$^+$ T cells transduced with retroviral vector (Myc-tagged) expressing GFP only (OE-CTL) or GAPDH (OE-GAPDH). Results were normalized to input RNA. **(D)** MERIP–qRT-PCR analysis of indicated mRNAs immunoprecipitated with anti-m^{6}A antibody in CD4$^+$ T cells cultured in vitro with IL-2 and IL-7 for 48 h from WT, VHL cKO, or DKO mice. Results were normalized to input RNA. **(E)** MERIP–qRT-PCR analysis of indicated mRNAs immunoprecipitated with anti-m^{6}A antibody in WT CD4$^+$ T cells cultured in the absence (Mock) or presence of 2.5 µM IAA. Results were normalized to input RNA. Each symbol (A) represents an individual mouse; small horizontal lines indicate the mean (± SD). *, P < 0.05; **, P < 0.01; ***, P < 0.001; ****, P < 0.0001; ns, nonsignificant (Student's t test). Data are representative of three independent experiments.

Table S1. **List of sequences of shRNAmir oligonucleotides**

shRNAmir	shRNAmir oligonucleotides (5′→3′)
shCD8	CTCGAGAAGGTATATTGCTGTTGACAGTGAGCGGCATCAGATGTAACAAATCAATAGTGAAGCCACAGATGTA
shScramble	CTCGAGAAGGTATATTGCTGTTGACAGTGAGCGACCATAGATGTTACCCTTTATTTAGTGAAGCCACAGATGTA
shItch	CTCGAGAAGGTATATTGCTGTTGACAGTGAGCGATCAAACAATATGAAACTTGAATAGTGAAGCCACAGATGTA
shPrdm1	CTCGAGAAGGTATATTGCTGTTGACAGTGAGCGCCGGAGCCATGAATCTCATTAATAGTGAAGCCACAGATGTA
shCD19	CTCGAGAAGGTATATTGCTGTTGACAGTGAGCGAAAGATGCAGACTCTTATGAAATAGTGAAGCCACAGATGTA
shCD14	CTCGAGAAGGTATATTGCTGTTGACAGTGAGCGAGCCTCTTTGTTTAAGGAACATTAGTGAAGCCACAGATGTA
shPdcd1	CTCGAGAAGGTATATTGCTGTTGACAGTGAGCGATCGGAGGATCTTATGCTGAACTAGTGAAGCCACAGATGTA
shBcl6	CTCGAGAAGGTATATTGCTGTTGACAGTGAGCGCGCTGTCAAAGAGAAGGCTTTATAGTGAAGCCACAGATGTA
shHif1a	CTCGAGAAGGTATATTGCTGTTGACAGTGAGCGAACACAGAAACTGAAGATCAACTAGTGAAGCCACAGATGTA
shHif2a	CTCGAGAAGGTATATTGCTGTTGACAGTGAGCGACGTGAGAACCTGACTCTCAAATAGTGAAGCCACAGATGTA
shEgln1	CTCGAGAAGGTATATTGCTGTTGACAGTGAGCGAGGCGTAACCCTCATGAAGTACTAGTGAAGCCACAGATGTA
shHk1	CTCGAGAAGGTATATTGCTGTTGACAGTGAGCGCGTGGTCAAGCTGCTGAATAAATAGTGAAGCCACAGATGTA
shFih	CTCGAGAAGGTATATTGCTGTTGACAGTGAGCGCCCATATAGAGTCATTACTAAATAGTGAAGCCACAGATGTA
shPdk1	CTCGAGAAGGTATATTGCTGTTGACAGTGAGCGAACAGACACAGTGATAAGGATCTAGTGAAGCCACAGATGTA
shLdha	CTCGAGAAGGTATATTGCTGTTGACAGTGAGCGACTTGTTGACGTCATGGAAGACTAGTGAAGCCACAGATGTA
shGpi1	CTCGAGAAGGTATATTGCTGTTGACAGTGAGCGCGGGCATATTCTGGTGGACTACTAGTGAAGCCACAGATGTA
shPfk-p	CTCGAGAAGGTATATTGCTGTTGACAGTGAGCGACCTCGTACTCAGAAACGAAAGTAGTGAAGCCACAGATGTA
shPfk-l	CTCGAGAAGGTATATTGCTGTTGACAGTGAGCGCGCCTACAATCTGCTCCAACACTAGTGAAGCCACAGATGTA
shGls	CTCGAGAAGGTATATTGCTGTTGACAGTGAGCGCGCCCTTGATCTCTATTTCCAGTAGTGAAGCCACAGATGTA
shAldoa	CTCGAGAAGGTATATTGCTGTTGACAGTGAGCGATGCCAGTATGTTACTGAGAAGTAGTGAAGCCACAGATGTA
shAlodc	CTCGAGAAGGTATATTGCTGTTGACAGTGAGCGCTCTCTCAACCTCAATGCCATCTAGTGAAGCCACAGATGTA
shGapdh	CTCGAGAAGGTATATTGCTGTTGACAGTGAGCGAACTGAGCATCTCCCTCACAATTAGTGAAGCCACAGATGTA
shPgk1	CTCGAGAAGGTATATTGCTGTTGACAGTGAGCGACTAGACAAAGTCAATGAGATGTAGTGAAGCCACAGATGTA
shPgam1	CTCGAGAAGGTATATTGCTGTTGACAGTGAGCGACGAGATGCTGGCTATGAATTTTAGTGAAGCCACAGATGTA
shEno1	CTCGAGAAGGTATATTGCTGTTGACAGTGAGCGAACTGTTGAGGTCGATCTGTACTAGTGAAGCCACAGATGTA
shPkm2	CTCGAGAAGGTATATTGCTGTTGACAGTGAGCGCGCTTTGCATCTGATCCCATTCTAGTGAAGCCACAGATGTA
shMct4	CTCGAGAAGGTATATTGCTGTTGACAGTGAGCGAGGTCTGGCTCTCAACTTCCAGTAGTGAAGCCACAGATGTA
shMpc1	CTCGAGAAGGTATATTGCTGTTGACAGTGAGCGCGCTATCAATGACATGAAGAAATAGTGAAGCCACAGATGTA
shPdha	CTCGAGAAGGTATATTGCTGTTGACAGTGAGCGAGCGGATCAGCTGTATAAGCAGTAGTGAAGCCACAGATGTA
shRictor	CTCGAGAAGGTATATTGCTGTTGACAGTGAGCGCTCACTTACTTTGCCTACTAAATAGTGAAGCCACAGATGTA
shRaptor	CTCGAGAAGGTATATTGCTGTTGACAGTGAGCGAAGTGTGAGTGTCAATGGAGATTAGTGAAGCCACAGATGTA
shOgdh	CTCGAGAAGGTATATTGCTGTTGACAGTGAGCGCGGACTTGTGCTGCTAAGTTAATAGTGAAGCCACAGATGTA
shSdha	CTCGAGAAGGTATATTGCTGTTGACAGTGAGCGCGCACTGGATCTTCTGATGGAATAGTGAAGCCACAGATGTA
shSdhb	CTCGAGAAGGTATATTGCTGTTGACAGTGAGCGAACAGAGGAACGCCTGGCCAAGTAGTGAAGCCACAGATGTA
shFh	CTCGAGAAGGTATATTGCTGTTGACAGTGAGCGCAGATTGGAGGTGCTACGGAACTAGTGAAGCCACAGATGTA
shAcly	CTCGAGAAGGTATATTGCTGTTGACAGTGAGCGCTCATTCAGTCTGTGTATGAAGTAGTGAAGCCACAGATGTA
shCpt1a	CTCGAGAAGGTATATTGCTGTTGACAGTGAGCGATGCCTCTATGTGGTGTCCAAGTAGTGAAGCCACAGATGTA
shIdh1	CTCGAGAAGGTATATTGCTGTTGACAGTGAGCGCTCTGACTACTTGAATACATTTTAGTGAAGCCACAGATGTA
shIdh2	CTCGAGAAGGTATATTGCTGTTGACAGTGAGCGCCGTGGGAAGCTGGATGGGAACTAGTGAAGCCACAGATGTA
shHk2	CTCGAGAAGGTATATTGCTGTTGACAGTGAGCGATCTCTGAAGCTGAGCCATGAATAGTGAAGCCACAGATGTA
shIdh3a	CTCGAGAAGGTATATTGCTGTTGACAGTGAGCGCACCTTGATACTGTATGTTTAATAGTGAAGCCACAGATGTA
shIdh3g	CTCGAGAAGGTATATTGCTGTTGACAGTGAGCGCCGTCATATCCGCATCATTAATTAGTGAAGCCACAGATGTA
shIdh3b	CTCGAGAAGGTATATTGCTGTTGACAGTGAGCGAATGCCCAATCTCTATGGCAACTAGTGAAGCCACAGATGTA
shPfk-fb3-1	CTCGAGAAGGTATATTGCTGTTGACAGTGAGCGACTGGAGCCTGTGATCATGGAATAGTGAAGCCACAGATGTA

Table S1. **List of sequences of shRNAmir oligonucleotides (*Continued*)**

shRNAmir	shRNAmir oligonucleotides (5′→3′)
shPfk-fb3-2	CTCGAGAAGGTATATTGCTGTTGACAGTGAGCGATCCAAGAAGCTGACTCGCTACTAGTGAAGCCACAGATGTA
shAco2	CTCGAGAAGGTATATTGCTGTTGACAGTGAGCGAGCCCACGGACTCAAGTGCAAGTAGTGAAGCCACAGATGTA
shMdh2	CTCGAGAAGGTATATTGCTGTTGACAGTGAGCGAACACGGGATGACCTGTTCAACTAGTGAAGCCACAGATGTA
shMettl3	CTCGAGAAGGTATATTGCTGTTGACAGTGAGCGCAGCTGCACTTCAGACGAATTATAGTGAAGCCACAGATGTA
shMettl14	CTCGAGAAGGTATATTGCTGTTGACAGTGAGCGCTGGGAGAGTATGCTTGCGAAATAGTGAAGCCACAGATGTA
shAlkbh5	CTCGAGAAGGTATATTGCTGTTGACAGTGAGCGATCCGTGTCTTTCTTCAGCGACTAGTGAAGCCACAGATGTA

Table S2. **List of primers used for qRT-PCR**

Gene	Forward primer (5′→3′)	Reverse primer (5′→3′)
β-actin	GCTGTGCTGTCCCTGTATGCCTCT	CCTCTCAGCTGTGGTGGTGAAGC
Vhl	GCTGCCTTTGTGGCTCAACTTCG	TGAGGGATGGCACAAACAGCTCC
Hk1	CGGAATGGGGAGCCTTTGG	GCCTTCCTTATCCGTTTCAATGG
Pfk-fb3	CCTACCCTGAGGAGTACGCA	CTCTTGGCGCTCTAATTCCA
Aldoa	TAGTCCTTTCGCCTACCCACC	CTCTGTCTGTTGCTGGGTGTT
Gapdh	TGTGTCCGTCGTGGATCTGA	CCTGCTTCACCACCTTCTTGA
Gpi1	GTTGCCTGAAGAGGCCAGG	GCTGTTGCTTGATGAAGCTGATC
Pgk1	ATTCTGCTTGGACAATGGAGC	AGGCATGGGAACACCATCA
Eno1	TGCGTCCACTGGCATCTAC	CAGAGCAGGCGCAATAGTTTTA
Pkm2	TTGCAGCTATTCGAGGAACTCCG	CACGATAATGGCCCCACTGC
Pdk1	GGACTTCGGGTCAGTGAATGC	TCCTGAGAAGATTGTCGGGGA
Pgam1	TCTGTGCAGAAGAGAGCAATCC	CTGTCAGACCGCCATAGTGT
Ldha	TGTCTCCAGCAAAGACTACTGT	GACTGTACTTGACAATGTTGGA
Mct4	TCACGGGTTTCTCCTACGC	GCCAAAGCGGTTCACACAC
Icos-1	CACGCTCTGTGCCTGAGTTAGTT	AGACTGAAGAACACTCCCGAGACA
Icos-2	CAGCTGAAGCTCTGGCTACC	TTAGGGTCATGCACACTGGA
Icos-3	TGAATACATGTTCATGGCGG	TCAGGGGAACTAGTCCATGC
Pdcd1	TGGTCATTCACTTGGGCTGT	AGAAGGTGAGGGACCTCCAG
Cxcr5	GCTAAGAGAATGACGACAGAGGTTCC	CTTGTACGGTTGGCTTGAGTGGTA
Bcl-6	CCTGTGAAATCTGTGGCACTCG	CGCAGTTGGCTTTTGTGACG
Foxo1	GTGGCTCTGTCCTGAAGAATCC	CATTAGGCTGCTCAAGGCTGAA
Il6ra	GAAGCATGCTGACCGTCG	GCTTGTCACTGTGCCATTTG
Tcf7	GCGGACATCAGCCAGAAG	TCACAGTATGGGGGAGCTGT
Lef1	AGCTGAGTGCACGCTAAAGG	GTATTTGGCCTGCTCTTCCC
Irf4	CCGTTGAAGAGGTAGGCTGAGGA	GGCGTTCCTGTGTCTGGCATAC
Prdm1	ACATAGTGAACGACCACCCCTG	CTTACCACGCCAATAACCTCTTTG
Tbx21	GCATGAAGCCCACACTCCTAC	ACTGGCCTTCGGTTTCCTTATC
Ascl2	GAGAGCTAAGCCCGATGGAG	CCCAGGTTTCTTGGGCTAGA
Klf2	CTAAAGGCGCATCTGCGTA	TAGTGGCGGGTAAGCTCGT
Ifng	CTTGGATATCTGGAGGAACTGG	GAATCAGCAGCGACTCCTTTTC
Tet1	CCGAATCAAGCGGAAGAATA	ACTTCAGGTTGCACGGTCTC
Tet2	AGCCCCATCACGTACAAAAC	TGTGGTGGCTGCTTCTGTAG
Tet3	CAGCAGCCGAGAAGAAGAAG	GGACAATCCACCCTTCAGAG
Dnmt1	GCTACCAGTGCACCTTTGGT	CAGAGGCAGCTTTTCTCCTG
Mettl3	CTCCGATGTTGATCTGGAGATAG	TGGACTGTTCCTTGGCTGTT
Mettl14	GATCCAAAGGCAGTTTTCCA	TGAATGAAGTCCCCGTCTGT